Effect of Anti-Inflammatory Protein Tnfα-Stimulated Gene-6 (TSG-6) on Rat Brain After Injury

Dr. Munqith Mazin Mghamis*, Dr. Maher Finjan Taher*, Dr. Haider Faisal Ghazi, Dr. Salih Mahdi Mustafa***

* University of Kufa/ College of Medicine/ Department of Anatomy
** Alnahrain University/ College of Medicine/ Department of Microbiology

Abstract

Background: This study proposes that the glial scar adjacent to the penetrating brain injuries is active in stabilizing the surrounding uninjured tissue by limiting the inflammatory response to the injury site. The study showed that tumor necrosis factor (TNF)-stimulated gene-6 (TSG-6), a well-known anti-inflammatory molecule, is present within the glial scar. The current study investigated the role of TSG-6 within the glial scar using TSG-6 *null* and littermate control rat subjected to penetrating brain injuries.

Results: The study outcomes display that rat lacking TSG-6 has a more severe inflammatory response after injury, which was correlated with an enlarged area of astrogliosis beyond the injury site.

Conclusion: The study results provide clue that TSG-6 has an anti-inflammatory role within the glial scar.

Keywords: TSG-6, Astrocytes, Glial scar, Inflammation and glycosaminoglycans**.**

Introduction

The traumatic brain injury (TBI) is a main medical distress that affects millions of people in the world each year [1, 2]. Many injuries can cause TBI resulting in a different range of injury severities [3–7]. With developed medical interventions in the last period, the mortality rate due to TBI has reduced, resulting in a significant number of people living with the long-term effects of TBI. It is well believed that in addition to the abrupt effects of TBI there are also many possible long-term gradually developing complications that are influenced by the type of injury, severity of the injury and medical interventions at the time of injury [8, 9]. Moreover, a link between mild traumatic brain injuries and Alzheimer's disease or chronic traumatic encephalopathy has long been suspected [10]. Recently, long-term effects of repeated TBI have been seen in multiple sports-related injuries, including post-traumatic Parkinsonism, post-traumatic dementia and chronic post-concussion syndrome [11–14]. Thus, reviewing the short- and long-term consequences of TBI at a cellular and molecular level may lead to a novel understanding and may be better long-term controlling of such injuries via new and/or refined treatment approaches.

Astrogliosis is a hallmark of TBI, which starts hours after injury and leads to an abnormal rise in the number of activated astrocytes in and around the injury site [15, 16]. In the acute phase that occurs immediately after injury, astrocytes are activated, becoming highly proliferative and up-regulating the production of extracellular proteins [17–19]. These astrocytes and their deposited extracellular matrix in and around the injury site form what is called a glial scar. A significant amount of evidence has established that the glial scar contains molecules, such as chondroitin sulfate proteoglycans (CSPGs) that delay axonal growth, thus inhibiting neuronal regeneration [15, 20–23]. The amount of the acute and chronic reactive astrogliosis, including the quantity and composition of the glial scar, affects immediate and long-term effects of TBI [6, 16, 24, 25]. Penetrating brain injuries (PBIs) cause direct parenchymal laceration, neuronal cell loss and hemorrhage, which lead to crucial tissue damage at the injury site. Astrogliosis is activated after TBIs forming a glial scar in and around the injury site [26–29]. Significantly, uninjured tissue around the injury site is also undergo

astrogliosis, and the process of glial scarring consequently extends beyond the injury site [30]. According to the fact that glial scarring restricts regeneration after injury, several studies have considered whether limiting astrogliosis after injury, with specific focus on limiting deposition, could potentially stimulate regeneration [23, 27, 31–34]. Although many researches were capable to establish positive effects of limiting glial scarring on neuronal regeneration, many others were inconclusive or actually found there was an increased inflammatory response terminating in tissue damage beyond the injury site and an increase in neuronal loss. Thus, rising evidence indicates that reactive astrocytes surrounding the injury site are influential in preserving the surrounding uninjured tissue by forming scar borders, which separate damaged and inflamed tissue from adjacent viable neural tissue [15, 16, 24, 35–40]. Sofroniew *et al.* vigorously confirmed that targeting astrocytes after brain and spinal cord injury leads to increased inflammation, delayed recovery and increased neuronal loss [39, 41–44]. Furthermore, the inhibition of astrocyte proliferation delays the healing period following central nervous system (CNS) injury [45]. Data from Hermann *et al.* illustrate that GFAP-driven ablation of STAT3 in astrocytes leads to the loss of lesion demarcation and successive glial scar formation, and, in turn, results in increased invasion of inflammatory cells into adjacent viable tissue and more spread of inflammation [46]. This proposes that early glial scar formation by astrocytes limits movement of inflammatory cells located within the injury site into adjacent healthy tissue, thereby limiting tissue damage to the injury site. Thus, recent evidence proposes scar tissue bordering the injury site is necessary for limiting inflammation and tissue damage to the injury site [37, 41]. There is an important number of researches investigating how reactive astrocytes regulate and restrict inflammation to the injury site, and which cellular machineries and major pathways could play a role in this process [20, 35, 41, 45, 47].

Recently, researchers found that tumor necrosis factor (TNF)- stimulated gene-6 (TSG-6) is secreted by astrocytes after injury and is a major constituent of the glial scar, but the role it plays within the glial scar remains to be recognized [48]. TSG-6 is a 35-kDa protein that is secreted by a wide variety of cell types in response to inflammatory mediators and growth factors [49], and was initially recognized as a gene product induced in fibroblasts by TNF [12]. TSG-6 contains a link module domain that mediates its interaction with the glycosaminoglycans (GAGs) hyaluronan (HA) and CS [49–51]. This study identified that TSG-6 is expressed in the CNS, where it catalyzes the transfer of heavy chains (HCs) from Inter-a-Inhibitor (IαI, also known as ITI) onto HA, forming a specialized HA/HC/TSG-6 matrix within the glial scar, but the role of this specialized matrix within the glial scar remains to be proven [48, 52–56]. This specific HA/HC/TSG-6 matrix has previously been shown to be monocyte-adhesive in other tissues and is believed to be present in most, if not all, inflammatory processes [57, 58]. These TSG-6 modified HA matrices bind inflammatory cells, and the interaction of these cells with this matrix controls their responses, which are central to pathological inflammation [59–65].

The main objective of this study was to investigate the role TSG-6, a component of the glial scar, has in astrogliosis after a PBI. As the well-characterized anti-inflammatory role of TSG-6 in other sites, the evidence of this study was that TSG-6 could participate in the formation of an immunosuppressive environment within the glial scar. The study findings show that *TSG-6 null* rats present a more severe inflammatory response and increased glial scar deposition after injury when compared to littermate control rats. This increased inflammatory response in *TSG-6 null* rats was correlated with an enlarged area of astrogliosis beyond the site of injury.

Materials and Methods

TSG6 null (TSG6−/−) or heterozygous (TSG6+/−) rats and animal maintenance

Transgenic Tsg-6 null mice (*Tnfp6Δ/Δ*), which is referred to as Tsg-6−/− rats, and heterozygous rats, which is referred to as Tsg-6+/− rats, were maintained as previously described [56]. Moreover, Tsg-6+/− rats have previously been shown not to display a phenotype and present similar TSG-6 expression levels as with rats, and were therefore used as littermate controls in previous study [56]. Experimental procedures for handling the rats were approved by the Institutional Animal Care and Use Committee (IACUC), University of Houston under protocol 16-036.

Brain injury

Rats (7 to 8 weeks old) were anesthetized with ketamine (80–100 mg/kg—Vedco INC, Catalog# 07-890- 8598) and xylazine (5–10 mg/kg, Akorn INC, Catalog# 07-808-1947) by IP injection and allowed to go into full anesthetic state. A sterile surgical drill (Precision Tools, Model Craft PPV2237) was used to

make a hole of approximately 1.5 mm in diameter in the skull over the right frontal cortex at the stereotaxic coordinates AP: 1.0 mm, ML: 1.5 mm, and DV: 1.5 mm, according to Franklin and Paxinos [85]. A 30-gauge needle (Exel, Catalog# 26437) was then used to make a puncture wound at a depth of 2 mm. After injury, the skin at the surgical site was closed with two sutures. The injured area was then cleaned with 70% ethanol, and rats were placed on a heating pad and monitored until they regained consciousness prior to being transferred to a clean cage. All surgeries were carried out at the same time of day to minimize bias. Rats were monitored daily and did not show any decrease in weight≥15% when compared to their pre-surgical weight. Rats were euthanized, as outlined below, at 1-, 3- and 5-days post injury to study the acute effects of brain injury, and at 10 and 14 days to study long-term/chronic effects. Five rats per experimental group were used for the real-time PCR analysis and at least seven rats per experimental group were used for immunofluorescence analysis.

Perfusion fixation and brain tissue processing

Brain samples were collected at 1, 3-, 5-, 10-, and 14-days post injury for immunofluorescence analyses. Briefly, rats were primarily injected with a lethal dose of combined anesthetics containing 200 mg of ketamine and 40 mg xylazine. Final dosage received was 3 mg of ketamine and 0.6 mg of xylazine per rat. Once rats were under deep anesthesia, abdominal and thoracic excisions were performed to expose the heart, which was used to perfuse 2% formalin (Fisher Scientific, Catalog# SF100-4) throughout the whole body via a gravity-driven flow system for whole body fixation. Subsequently, the brain was isolated from the skull and further immerse fixed for 2 days in 2% paraformaldehyde (Electron Microscopy Sciences, Catalog# 15710). For cryosection processing, brains were immersed in 30% sucrose for 2 days, embedded in OCT embedding medium (Fisher Healthcare, Catalog# 4585) and frozen. Sections 10 μm thick were obtained, mounted on super frost slides (VWR, Catalog# 48311-703) and stored at−20 °C until use.

Immunofluorescence

During their use, the slides were heated at 65 °C for 30 min and, then, sections were washed with PBS to remove tissue freezing medium. Sections were then treated with 0.1% glycine (Fisher Chemical, Catalog# G46-500), blocked with 5% FBS (Seradigm, Catalog# 3100-500) and permeabilized with 0.1% saponin prepared in PBS. Sections were, subsequently, incubated with the primary antibodies anti-Tenascin (Abcam, Ab108930), anti-GFAP (Abcam, Ab4647), anti-CD68 (Abcam, Ab31630) and anti-β III tubulin (Covance, PRB435P-100). Sections were washed and incubated with appropriate secondary donkey antibodies conjugated with Alexa Fluor® 488 (Life Technologies) or Alexa Fluor® 555 (Life Technologies) for one hour at 18 °C. For HA staining, tissues were incubated with biotinylated HA binding protein (385911, Millipore) followed by NeutrAvidin®Alexa 555 (Life Technologies). The tissues were then washed and nuclei stained with 4',6-diamidino-2-phenylindole (DAPI, Sigma-Aldrich). Sections were mounted in Prolong®Gold (Molecular Probes) and imaged using a ZEISS LSM 800 Confocal microscope with Airyscan. Secondary controls were done with a goat IgG isotype control (ab37388; Abcam) in place of the primary antibody and did not yield any significant staining. For imaging, multiple z-stack tiles were captured of entire brain sections and frames were processed together into a single image (using the stitching mode followed by full orthogonal projection) using Zen Software (Zeiss). The number of GFAP+ and CD68+ cells in and around the injury site were counted by two independent investigators in a blinded manner and the relative fluorescent intensity was measured using the Zen Software (Zeiss). At least 2 sections were scanned and analyzed from each animal for each set of antibodies and representative images shown in the figures.

RNA extraction from brains and real-time PCR analysis

Brains collected from injured rats at 1-, 5- and 10-days post injury were used for RNA extraction. At least 5 rats were used per experimental group and each animal was analyzed separately. Briefly, rats were euthanized and brain tissue was immediately isolated from each rat. Injury sites (A samples) were dissected from the rest of the injured right hemisphere, transferred into a labeled Eppendorf tube and immediately immersed in liquid nitrogen. The remaining right hemisphere brain tissue (B samples) from each animal was transferred into a different tube and frozen as described. The samples were kept at−80 °C until RNA extraction. Total RNA was isolated from these tissue samples using Trizol® Reagent (Invitrogen, Carlsbad, CA) and chloroform extraction (Sigma-Aldrich, Catalog# 650498). First strand cDNA was reverse transcribed using 1.5 to 2 μg of total RNA and the high-capacity cDNA

Reverse Transcription kit (Applied Biosystems, catalog# 4368814, lot 00593854), according to the manufacturer's instructions. Quantitative real-time PCR amplification was performed on 1 µg or 50 ng of the cDNA (1:5) using the Power Up SYBR Green Master Mix kit (Applied Biosystems, Catalog# A25918) in a CXF Connect Real-time System from BIO-RAD, using an activation cycle of 95 °C for 10 min, 40 cycles of 95 °C for 15 s and 60 °C for 1 min.

Statistical analysis

All values are presented as the mean ± standard deviation of the mean. The difference between the two groups was compared by means of the Student's t-test. $p \leq 0.05$ was considered to be statistically significant. Statistical analysis was performed using the GraphPad Prism version 7 software package (GraphPad Software, San Diego, CA, USA). * Was used to indicate statistical differences of≤0.05. Unless indicated otherwise, * indicates the statistical difference of Tsg-6−/− rats compared to Tsg-6+/− rats for each time point.

Results

TSG-6 expression after PBI

In this study, transgenic *Tsg-6 null* rats, will be referred to as *Tsg-6*−/− rats, and heterozygous rats, will be referred to as *Tsg-6*+/− rats, were used to explore the role of TSG-6 in the glial scar. In order to explore whether TSG-6 is present in the glial scar after brain injury, we studied the expression profile of *Tsg6* in the injury site and injured hemisphere before and after a PBI in *Tsg-6*+/− rats (Fig. 1A). There was a twofold increase in *Tsg-6* expression 5 days after injury when compared to uninjured rats. There was a further increase in *Tsg-6* expression over time after injury, with expression increasing twofold from 5 to 10 days after injury (Fig. 1A). Remarkably, we did not find a difference in the expression levels of *Tsg-6* between the injury site and the remaining hemisphere, indicating that *Tsg*-6 expression is not contained exclusively to the injury site (Fig. 1A). Therefore, there is also an increase in *Tsg-6* expression in the surrounding tissue after injury. No *Tsg-6* expression was recognized in any of the samples from Tsg-6−/− rats indicating that these rats are certainly null for Tsg-6.

Analysis of astrocyte recruitment after PBI

The study measured the level of astrogliosis in the injury site and in the remaining injured hemisphere by calculating the levels of GFAP+ astrocytes using real-time PCR (Fig. 1B, C). Therefore, mRNA was isolated from the injury site and remaining injured hemisphere 1 and 5 days after injury of *Tsg-6*−/− and *Tsg-6*+/− rats. Both *Tsg-6*−/− and *Tsg-6*+/− rats displayed an increase in the levels of GFAP expression in the injury site when compared to the remaining injured hemisphere, which documents literature [36, 63, 64]. *Tsg-6*−/− rats showed a significant increase in GFAP levels within the injury site at both 1- and 5-days after injury when compared to *Tsg-6*+/− rats (Fig. 1B, C).

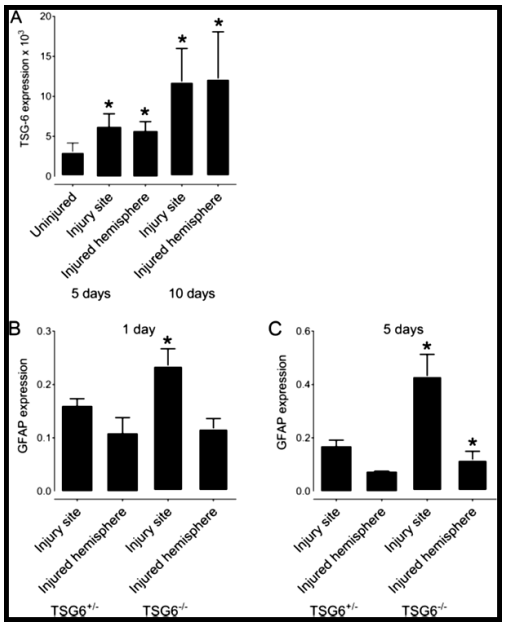

Fig. 1 TSG-6 and GFAP expression after PBI. TSG-6 and GFAP mRNA expressions were quantified in the injury site and the injured hemisphere after PBI. A *TSG*+/− rats were subjected to PBI, and the injury site and remaining injured hemisphere were collected 5 and 10 days after injury for analysis of TSG-6

expression. B, C *TSG*+/− and *TSG-6*−/− rats were subjected to PBI, and the injury site and remaining injured hemisphere were collected 1 day (B) and 5 days (C) after injury for analysis of GFAP expression. * = $p \leq 0.05$ comparing *TSG-6*−/+ and *TSG-6*−/− rats.

This data indicates that *Tsg-6*−/− rats have more astrocytes in the injury site when compared to *Tsg-6*+/− rats. At 5 days after injury, there was a significant increase in GFAP expression in the injured hemisphere of *Tsg-6*−/− rats compared to *Tsg-6*+/− rats, indicating that *Tsg-6*−/− rats present astrogliosis beyond the injury site at 5 days after injury.

The effect of TSG-6 on the secretion of inflammatory markers after PBI

The inflammatory response was also assessed in *Tsg-6*−/− and *Tsg-6*+/− rats 1, 5 and 10 days after injury by calculating the expression levels of *NFκB, Rantes* and *IL1β* (Fig. 2). Higher expression levels of *NFκB, Rantes* and *IL1β* were illustrated in *Tsg-6*−/− rats when compared to *Tsg-6*+/− rats during the acute phase after injury. Specifically, a ~ 2.5-fold and threefold increase in *NfκB* expression was found in the injury site and remaining injured hemisphere, respectively, in *Tsg-6*−/− rats compared to *Tsg-6*+/− rats 5 days after injury (Fig. 2B). 10 days after injury there was still a significant increase in *NfκB* expression in the surrounding hemisphere of *Tsg-6*−/− rats when compared to *Tsg-6*+/− rats (Fig. 2C). No significant differences were found in the expression of *NfκB* between *Tsg-6*−/− and *Tsg-6*+/− rats 1 day after injury (Fig. 1A). The levels of *Ccl5* (*Rantes)* were also evaluated 1-, 5- and 10-days after injury. There was a significant increase in the expression of *Rantes* in the injured hemisphere of *Tsg-6*−/− rats when compared to *Tsg-6*+/− rats (a fourfold increase) 5 days after injury; however, no difference was found between *Tsg-6*−/− and *Tsg-6*+/− rats 1 and 10 days after injury (Fig. 2D–F). *IL1β* levels were increased in the injury site of *TSG-6*−/− rats when compared to *Tsg-6*+/− rats at 1 day after injury (Fig. 2G). At 5 days after injury a threefold and fourfold increase in the expression of *IL1β* were noted in the injury site and remaining injured hemisphere, respectively, of *Tsg-6*−/− rats when compared to *Tsg-6*+/− rats (Fig. 2H). At 10 days after injury, a 2.5-fold increase in the expression of *IL1β* was noted in the injury site of *Tsg-6*−/− rats when compared to *Tsg-6*+/− rats (Fig. 2I).

The effect of TSG-6 on the activation of microglia and infiltration of macrophages into the injury site after PBI

In order to evaluate the inflammatory response in *Tsg-6*−/− and *Tsg-6*+/− rats, the number of CD68+ cells present within the injury site at 3 days after injury, was also evaluated (Fig. 3A, C). CD68 is usually used as a marker for macrophages and activated microglia. There was a significant increase in the number of CD68+ cells in and around the injury site of *Tsg-6*−/− rats when compared to *Tsg-6*+/− rats (Fig. 3A panels *i* and *ii*). Prominently, even when analyzing deeper regions of the injury site of *Tsg-6*+/− rats, the level of CD68+ cell infiltration was not as strong as that observed in *Tsg-6*−/− rats (Fig. 3A panel *iii*). The combined number of CD68+ cells in the injury site and within a range of 100 μm from the wound edge was calculated from images obtained from 2 different sections from at least 5 rats from each experimental point (Fig. 3C). A twofold increase in CD68+ cells was found in *Tsg-6*−/− rats when compared to *Tsg-6*+/− rats (Fig. 3C).

Correlation between increased inflammatory response and neuronal damage

In order to verify whether the increased inflammatory response observed in *Tsg-6*−/− rats correlates with neuronal loss, the distribution of neurons in and around the injury site was analyzed in *Tsg-6*−/− and *Tsg-6*+/− rats 14 days after injury (Fig. 3B). Therefore, β III tubulin was used as a tissue-specific marker for detecting neurons within injured and non-injured brains. The distribution of β III tubulin can be seen in the equivalent region of uninjured *Tsg-6*−/− and *Tsg-6*+/− rats (Fig. 3 B panels *I* and *ii*). A significant increase in the area devoid of β III tubulin staining can be detected in and around the injury site of *Tsg-6*−/− rats when compared to *Tsg-6*+/− rats 14 days after injury (Fig. 3B *iii* and *iv*). The relative fluorescence units (RLU) were calculated from an image of the injury site captured from at least 3 rats per experimental point. There was a fourfold decrease in β III tubulin staining in and around the injury site of *Tsg-6*−/− rats when compared to *Tsg-6*+/− rats 14 days after injury (Fig. 3D).

The effect of TSG-6 on the secretion of glial scar components after PBI

Glial scar secretion was also assessed within the injury site and injured hemisphere by measuring the expression levels of the biosynthetic enzymes responsible for HA and CS chain elongation, specifically hyaluronan synthase 2 (*Has2*),

carbohydrate (chondroitin 4) sulfotransferase (*chst 11*) and carbohydrate (chondroitin 4) sulfotransferase 12 (*chst 12*) (Fig. 4). *Has2* expression increased in the injury site when compared to the remaining injured hemisphere 5 days after injury in both *Tsg-6*+/− and *Tsg-6*−/− rats, indicating the several previously published studies showing that HA is an integral component of the glial scar [17, 66–68]. Remarkably, there was a twofold increase in *Has2* expression in the injury site of *Tsg-6*−/− rats when compared to *Tsg-6*+/− rats 5 days after injury, indicating that there is a higher rate of glial scar production in *Tsg-6*−/− rats when compared to *Tsg-6*+/− rats (Fig. 4A). At 10 days post-injury, *Has2* expression was still increased by twofold in *Tsg-6*/− rats when compared to *Tsg-6*+/− rats, but at this time point there was also an increase in *Has2* expression in the remaining injured hemisphere of *Tsg-6*−/− rats when compared to *Tsg-6*+/− rats (Fig. 4B). Thus, at 10 days after injury, in *Tsg-6*−/− rats, the expression of glial scar components was no longer limited to the injury site, but was also existing within the remaining injured hemisphere. Remarkably, this was also true for the expression of *Chst11* and *Chst12*, which showed a fivefold and fourfold increase, respectively, within the injured hemisphere of *Tsg-6*−/− rats at 5 days after injury when compared to *Tsg-6*+/− rats (Fig. 4C, E). The increase in *Chst11* and *Chst12*, in both the injury site and injured hemisphere, was continued through to 10 days after injury (Fig. 4D, F).

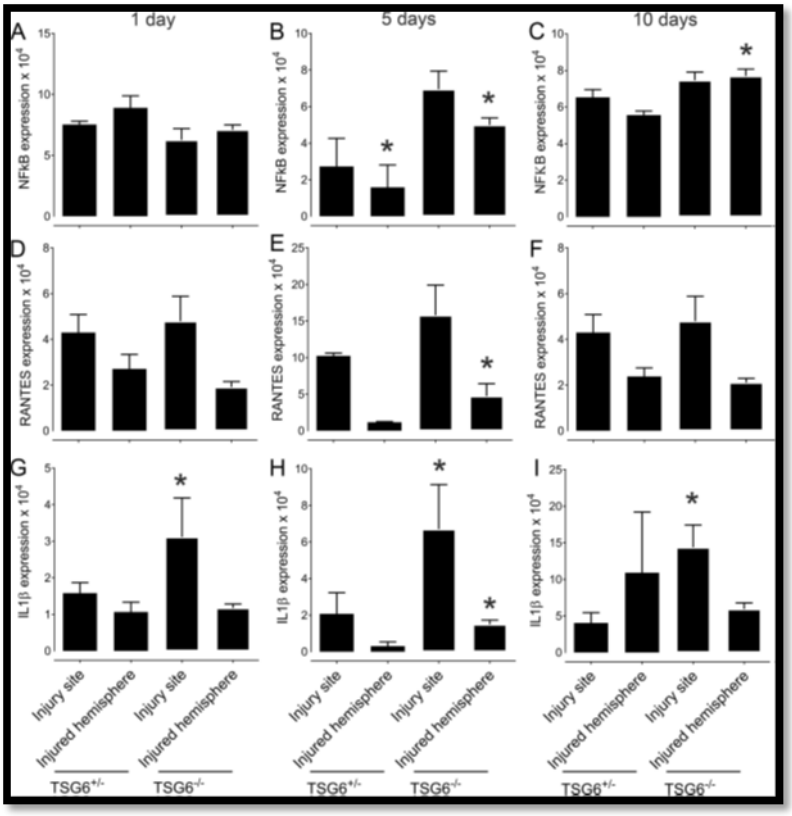

Fig. 2 Analysis of inflammatory markers after PBI. NFκB, RANTES and IL1β mRNA expressions were quantified in the injury site and the injured hemisphere after PBI. *TSG*+/− rats and *TSG-6*−/− rats were subjected to PBI and the injury site and remaining injured hemisphere were collected 1, 5 and 10 days after injury. mRNA was extracted and subjected to real-time PCR analysis for NFκB (A–C), RANTES (D–F) and IL1β (G–I) mRNA expression. * = $p \leq 0.05$ comparing *TSG-6*−/+ and *TSG-6*−/− rats

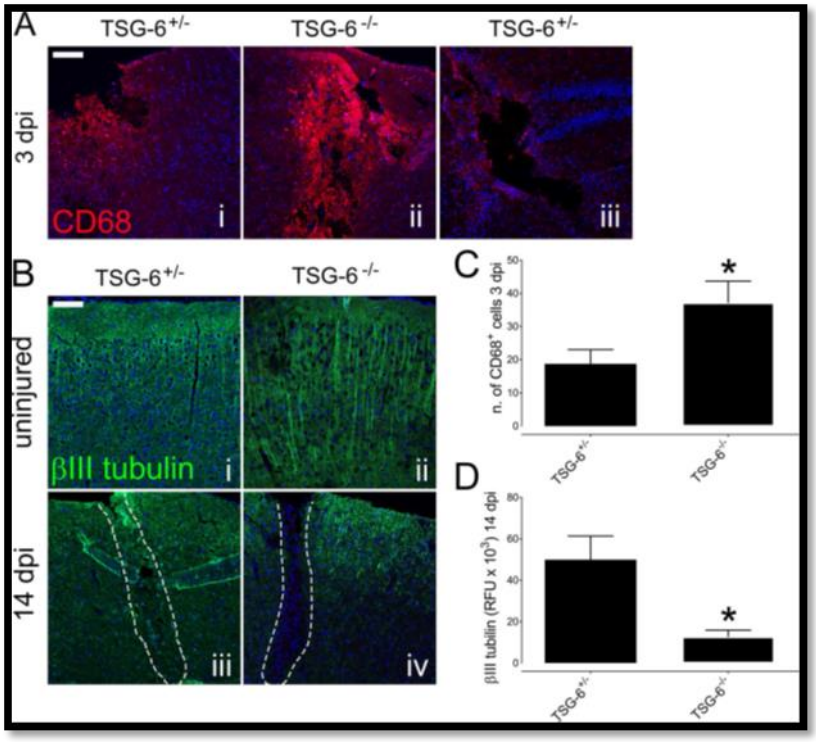

Fig. 3 Analysis of inflammatory cell infiltration and neuronal cell loss after PBI. The distribution of macrophages and activated microglia was

evaluated within the injury site of *TSG*+/− and *TSG-6*−/− rats 3 days post-injury (dpi) by anti-CD68 immunostaining (red) (A). Neuronal cells were immunostained with anti-β III tubulin (green) in the equivalent area of uninjured *TSG*+/− (*i*) and *TSG-6*−/− (*ii*) rats and within the injury site of

TSG-6−/+ (*iii*) and *TSG-6*−/− (iv) rats 14 days post-injury (dpi). The number of CD68+ cells was counted in the injury site and within 100 μm of the wound edge of *TSG-6*−/+ and *TSG-6*−/− rats 3 days post-injury (C). The relative fluorescent units (RFU) of anti-β III tubulin staining were quantified in and around the injury site of *TSG-6*−/+ and *TSG-6*−/− rats 14 days post-injury (D). Nuclei were counterstained with DAPI. Scale bar represents 100 μm. * = $p \leq 0.05$ comparing *TSG-6*−/+ and *TSG-6*−/− rats.

The effect of TSG-6 on activation and recruitment of astrocyte after PBI

For more examination of the process of astrogliosis in *Tsg-6*+/− and *Tsg-6*−/− rats, injured brains were picked and processed for histology. Sections were stained for GFAP in order to evaluate the distribution of astrocytes in and around the injury site, and, also, throughout the outstanding brain tissue. The number of astrocytes (GFAP+ cells) was calculated within the injury site, throughout the injured hemisphere, and all over the contralateral hemisphere 3- and 14-days post-injury (Fig. 5A, B). At 3 and 14 days postinjury there was a significant increase in the number of astrocytes within the injury site when compared to the injured hemisphere and contralateral hemisphere in both *Tsg-6*+/− and *Tsg-6*−/− rats. At 3 days postinjury there was no significant difference between the number of astrocytes within the injury site between *Tsg-6*+/− and *Tsg-6*−/− rats; however, there was a significant increase in the number of astrocytes within the injured hemisphere in *Tsg-6*−/− rats when compared to *Tsg-6*+/− rats (Fig. 5A). At 14 days post-injury there was a significant increase in the number of astrocytes within the injury site and injured hemisphere in *Tsg-6*−/− rats when compared to *Tsg-6*+/− rats (Fig. 5B, D). The increase in astrocytes can be seen outside the injury site in *Tsg-6*−/− rats (Fig. 5C, D panel iv).

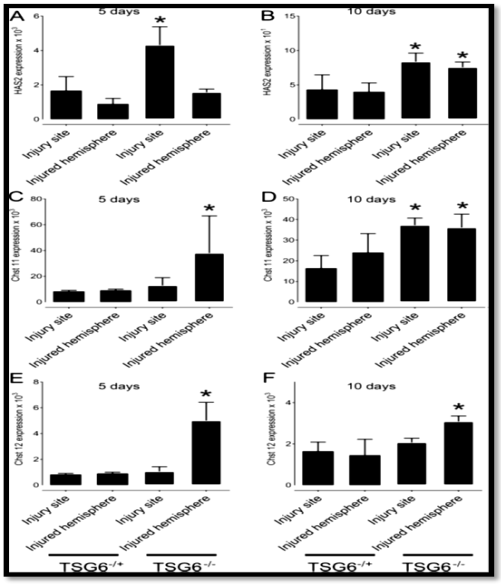

Fig. 4 Analysis of glial scar extracellular matrix components after PBI. HAS2, Chst 11 and Chst 12 mRNA expression levels were quantified in the injury site and the injured hemisphere after PBI. *TSG*+/− and *TSG-6*−/− rats were subjected to PBI, and the injury site and remaining injured hemisphere were collected 5 and 10 days after injury. mRNA was extracted and subjected to real-time PCR analysis for HAS2 (A, B), Chst11 (C, D) and Chst 12 (E, F) mRNA expression. * = $p \leq 0.05$ comparing *TSG-6*−/+ and *TSG-6*−/− rats

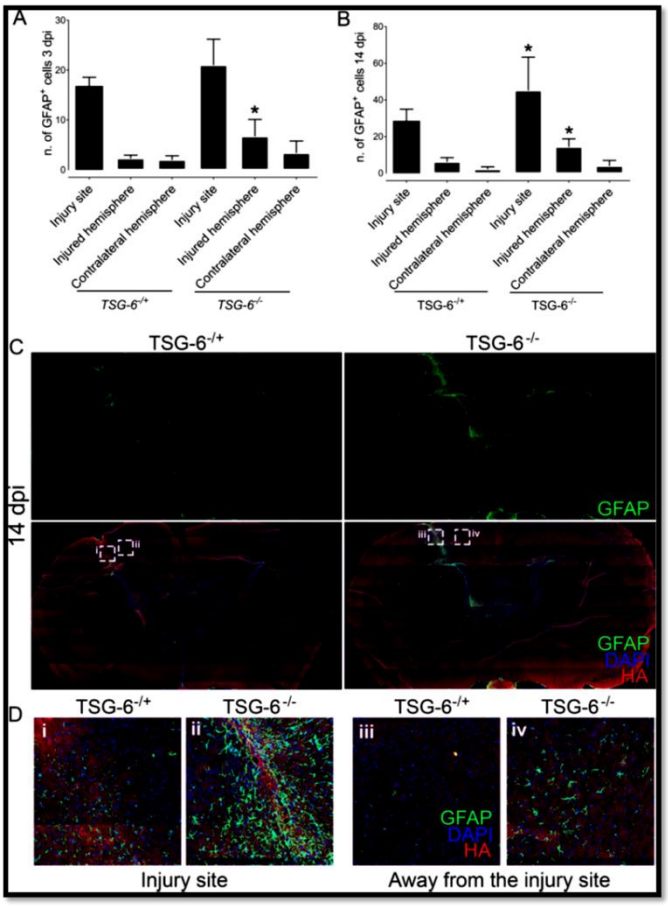

Fig. 5 Analysis of astrocyte activation and recruitment after PBI. Brain sections from *TSG-6*+/− and *TSG-6*−/− rats were analyzed by immunofluorescence. Astrocytes were identified with anti-GFAP (green) and the glial scar with HABP (red). Nuclei were counterstained with DAPI (blue). Z-stacks were captured of the entire brain section using the tilling mode, and images were stitched

together using Zen software. Thereafter, the number of astrocytes was counted within the injury site, within the injured hemisphere and in the contralateral hemisphere of brains 3 (A) and 14 dpi (B) in a double blinded manner. The distribution of astrocytes throughout the brain sections shows that in *TSG-6*−/− rats the increase in astrocytes is not restricted to the injury site (C). Magnified images of the areas demarcated in (C) can be seen in (D). At least 3 rats were analyzed per genotype for each time point. * = $p \leq 0.05$ comparing *TSG*+/− and *TSG-6*−/− rats.

Discussion

The most recognizable extracellular matrix components in the central nervous system are Chondroitin sulfate proteoglycans (CSPGs) [69]. Ten years ago, Silver *et al.* recognized that CSPGs within the glial scar inhibit axonal growth, and this triggered a great deal of interest in targeting CS within the scar tissue as a means to promote axonal regeneration [32, 70–72]. Then after, strategies using the enzymes chondroitinase ABC (ChABC) and ChAC have been used to remove the CS component of the glial scar as means to promote axonal growth and regeneration [50, 73–77]. Numerous studies have shown that specifically removing CS within the glial scar is adequate for axons to grow across the injury site [32, 70, 78, 79]. However, significant regeneration was never observed in these studies, and many groups found limited or no improvement after targeting CS within the glial scar [70]. One unique characteristic of TSG-6 is its known ability to bind to a number of ligands including HA, CS and core proteins of proteoglycans (i.e., versican and aggrecan), forming specific HA/HC/TSG-6 and/or CS/HA/HC/TSG-6 matrices with immunosuppressive characteristics [61, 80–84]. So, given that TSG-6 directly binds to both HA and CS to form specific anti-inflammatory matrices, the ChABC and ChAC treatments used over the years to target the glial scar as a means to promote regeneration would also have removed TSG-6, a known anti-inflammatory molecule that is also a component of the glial scar [82]. The loss of TSG-6 by these treatments could, partially, explain why significant functional recovery was never got after ChABC and/or ChAC treatments. To discover the role of TSG-6 in TBI, specifically in astrogliosis, this study compared the differences in injury outcomes in *Tsg-6*−/− and *Tsg-6*+/− rats after PBIs. This study shows an increase in TSG-6 expression in the injured hemisphere of *Tsg-6*+/− rats after TBI. This increase in expression of TSG-6 after CNS insults supports the previous findings that astrocytes secrete high levels of TSG-6 upon injury, which aids in the formation of a specialized HA/HC/TSG-6 matrix as part of an inflammatory response [48]. Since TSG-6 is known for having anti-inflammatory properties, to further study whether high levels of TSG-6 serve a purpose of rapidly suppressing inflammation after injury, in this study made similar penetrating injuries in *Tsg-6*−/− rats. The study used immunofluorescence and RNA expression analyses of inflammatory and glial scar markers to explain the outcome during the acute phase and chronic phase of TBI. During the acute phase after injury, the observed increase in astrocyte activation, inflammatory cell infiltration and expression of inflammatory cytokines in *Tsg-6*−/− rats indicate that the loss of TSG-6 results in a greater inflammatory response. Moreover, during the chronic phase of injury, unrestricted inflammatory response was observed throughout the injured hemisphere and was not limited to the injury site, as is seen after normal glial scar formation. Thus, injured *Tsg-6*−/− rats appear to test more severe tissue damage than their *Tsg-6*+/− counterpart, both within and around the injury site. Thus, the loss of TSG-6 allows the damage to spread from the injury site to neighboring healthy tissues. The study suggest that the cause of such widespread damage is due to the lack of the specialized HA-TSG6 or HA/HC/TSG-6 matrix, which could possibly serve to stabilize the glial scar and form an immunosuppressive environment, thereby protecting adjacent tissue from further damage. This hypothesis is further supported by the increase in CSPG and HA biosynthesis, both glial scar components, in *Tsg-6*−/− rats. Specifically, these rats show increased *Has2*, *Chst11* and *Chst12* expression levels in tissues collected after the onset of glial scarring, and, also, during the chronic phase of astrogliosis, indicating an increase in scar tissue formation. This increase in expression was not only observed at the injury site, but also throughout the whole injured hemisphere, suggesting that the tissue damage spreads beyond the injury site in the absence of TSG-6. All these results demonstrate that the loss of TSG-6 leads to a more severe inflammatory response and, consequently, increased scarring after TBI.

Thus, these results support the hypothesis put forward by many groups over the past decade that preventing the formation of the glial scar leads to inflammation and damage beyond the injury site. The study also provides experimental evidence that shows that the glial scar acts to restrict the damage to the injury site. Significantly, these findings should be taken into account when attempts are made to disrupt

the glial scar as a means to promote neuronal regeneration, since preventing formation of the glial scar may not have the beneficial outcomes as previously supposed.

Conclusion

The results of this study show that TSG-6 has an anti-inflammatory role in the glial scar. The study further supports the hypothesis that the glial scar forms a protective border surrounding the injury site thereby preventing the spread of inflammation and damage beyond the injury site.

References

1. Hayder A.A., Wunderlich CA, Puvanachandra P, Gururaj G, Kobusingye OC. The impact of traumatic brain injuries: a global perspective. Neuro Rehabilitation. 2007; 22:341–53.
2. Bose P, Hou J, Thompson FJ. Traumatic brain injury (TBI)-induced spasticity: neurobiology, treatment, and rehabilitation. Brain Neurotrauma: Molecular, Neuropsychological, and Rehabilitation Aspects. 2015.
3. Blennow K, Brody DL, Kochanek PM, Levin H, McKee A, Ribbers GM, et al. Traumatic brain injuries. Nat Rev Dis Prim. 2016; 2:1–19.
4. Graham DI, Mcintosh TK, Maxwell WL, Nicoll JAR. Recent advances in neurotrauma. J Neuropathol Exp Neurol. 2000; 59:641–51.
5. Zaninotto ALC, Costa BT, Ferreira IS, French M, Paiva WS, Fregni F. Traumatic brain injury. In: Neuromethods. 2018.
6. Burda JE, Bernstein AM, Sofroniew MV. Astrocyte roles in traumatic brain injury. Exp Neurol. 2016; 275:305–15.
7. Gugliandolo E, D'Amico R, Cordaro M, Fusco R, Siracusa R, Crupi R, et al. Neuroprotective effect of artesunate in experimental model of traumatic brain injury. Front Neurol. 2018; 9:590.
8. Kovacs SK, Leonessa F, Ling GSF. Blast TBI models, neuropathology, and implications for seizure risk. Front Neurol. 2014; 5:47.
9. Sharp DJ, Scott G, Leech R. Network dysfunction after traumatic brain injury. Nat Rev Neurol. 2014; 10:156–66.
10. Fakhran S, Alhilali L. Neurodegenerative changes after mild traumatic brain injury. In: Concussion. 2012.
11. Nagahiro S, Mizobuchi Y. Current topics in sports-related head injuries: a review. Neurol Med Chir (Tokyo). 2014.
12. Jordan BD. The clinical spectrum of sport-related traumatic brain injury. Nat Rev Neurol. 2013; 9:222–30.
13. Costanza A, Weber K, Gandy S, Bouras C, Hof PR, Giannakopoulos P, et al. Review: contact sport-related chronic traumatic encephalopathy in the elderly: clinical expression and structural substrates. Neuropathology Applied Neurobiology. 2011; 27:570–84.
14. McAllister T, McCrea M. Long-term cognitive and neuropsychiatric consequences of repetitive concussion and head-impact exposure. J Athletic Training. 2017; 52:309-17.
15. Sofroniew MV, Vinters HV. Astrocytes: biology and pathology. Acta Neuropathology. 2010; 119:7-53.
16. Sofroniew MV. Astrogliosis. Cold Spring Harb Perspect Biol. 2015. 7.
17. George N, Geller HM. Extracellular matrix and traumatic brain injury. J Neurosci Res. 2018; 96:573–88.
18. Siracusa R, Fusco R, Cuzzocrea S. Astrocytes: role and functions in brain pathologies. Front Pharmacol. 2019; 10:1114.
19. Zhou Y, Shao A, Yao Y, Tu S, Deng Y, Zhang J. Dual roles of astrocytes in plasticity and reconstruction after traumatic brain injury. Cell Commun Signal. 2020; 18:1–16.
20. Sofroniew MV. Reactive astrocytes in neural repair and protection. Neuroscientist. 2005 .11:400-7
21. Smith PD, Coulson-Thomas VJ, Foscarin S, Kwok JCF, Fawcett JW. "GAG ing with the neuron": the role of glycosaminoglycan patterning in the central nervous system. Exp Neurol. 2015; 274:100–14.
22. McGraw J, Hiebert GW, Steeves JD. Modulating astrogliosis after neurotrauma. Journal of Neuroscience Researches 2001; 63:109–15.
23. Kawano H, Kimura-Kuroda J, Komuta Y, Yoshioka N, Li HP, Kawamura K, *et al.* Role of the lesion scar in the response to damage and repair of the central nervous system. Cell Tissue Researches 2012; 349:169–80.
24. Burda JE, Sofroniew MV. Reactive gliosis and the multicellular response to CNS damage and disease. Neuron. 2014; 81:229–48.
25. Sofroniew MV. Molecular dissection of reactive astrogliosis and glial scar formation. Trends Neuroscience. 2009; 32:638–47.
26. Okada S, Hara M, Kobayakawa K, Matsumoto Y, Nakashima Y. Astrocyte reactivity and

astrogliosis after spinal cord injury. Neuroscience Researches. 2018; 43:126-39.
27. Davies SJA, Goucher DR, Doller C, Silver J. Robust regeneration of adult sensory axons in degenerating white matter of the adult rat spinal cord. Journal of Neuroscience. 2018; 19:5810–22.
28. McKeon RJ, Jurynec MJ, Buck CR. The chondroitin sulfate proteoglycans neurocan and phosphacan are expressed by reactive astrocytes in the chronic CNS glial scar. Journal Neuroscience. 2018; 19:10778–88.
29. Okada S, Nakamura M, Katoh H, Miyao T, Shimazaki T, Ishii K, *et al*. Conditional ablation of Stat3 or Socs3 discloses a dual role for reactive astrocytes after spinal cord injury. Nat Med. 2006; 12:829–34.
30. Fitch MT, Doller C, Combs CK, Landreth GE, Silver J. Cellular and molecular mechanisms of glial scarring and progressive cavitation: In vivo and in vitro analysis of inflammation-induced secondary injury after CNS trauma. Journal of Neuroscience. 1999; 19:8182–98.
31. Vogelaar CF, König B, Krafft S, Estrada V, Brazda N, Ziegler B, *et al*. Pharmacological suppression of CNS scarring by deferoxamine reduces lesion volume and increases regeneration in an in vitro model for astroglial-fibrotic scarring and in rat spinal cord injury in vivo. PLoS ONE. 2015; 10: e0134371.
32. Silver J, Miller JH. Regeneration beyond the glial scar. Natural Review of Neuroscience. 2004; 5:146–56.
33. Galtrey CM, Fawcett JW. The role of chondroitin sulfate proteoglycans in regeneration and plasticity in the central nervous system. Brain Research Review. 2007; 54:1–18.
34. Lin CM, Lin JW, Chen YC, Shen HH, Wei L, Yeh YS, Chiu WT. Hyaluronic acid inhibits the glial scar formation after brain damage with tissue loss in rats. Surgical Neurology. 2009; 72: S50–4.
35. Gesteira TF, Coulson-Thomas YM, Coulson-Thomas VJ. Anti-inflammatory properties of the glial scar. Neural Regenerative Researches. 2016; 11:1742.
36. Voskuhl RR, Peterson RS, Song B, Ao. Y, Morales LBJ, Tiwari-Woodruff S, *et al*. Reactive astrocytes form scar-like perivascular barriers to leukocytes during adaptive immune inflammation of the CNS. Journal of Neuroscience. 2009; 29:11511–22.
37. Wanner IB, Anderson MA, Song B, Levine J, Fernandez A, Gray-Thompson Z, *et al*. Glial scar borders are formed by newly proliferated, elongated astrocytes that interact to corral inflammatory and fibrotic cells via STAT3-dependent mechanisms after spinal cord injury. Journal of Neuroscience. 2013; 33:12870–86.
38. Faulkner JR. Reactive astrocytes protect tissue and preserve function after spinal cord injury. Journal of Neuroscience. 2004; 24:2143–55.
39. Myer DJ, Gurkoff GG, Lee SM, Hovda DA, Sofroniew MV. Essential protective roles of reactive astrocytes in traumatic brain injury. Brain. 2006; 129:2761–72.
40. Fitch MT, Silver J. CNS injury, glial scars, and inflammation: inhibitory extracellular matrices and regeneration failure. Experimental Neurology. 2008; 209:294–301.
41. Bush TG, Puvanachandra N, Horner CH, Polito A, Ostenfeld T, Svendsen CN, *et al*. Leukocyte infiltration, neuronal degeneration, and neurite outgrowth after ablation of scar-forming, reactive astrocytes in adult transgenic mice. Neuron. 1999; 23:297–308.
42. Wilhelmsson U. Absence of glial fibrillary acidic protein and vimentin prevents hypertrophy of astrocytic processes and improves post-traumatic regeneration. Journal of Neuroscience. 2004; 24:5016–21.
43. Pekny M, Johansson CB, Eliasson C, Stakeberg J, Wallen A, Perlmann T, *et al*. Abnormal reaction to central nervous system injury in mice lacking glial fibrillary acidic protein and vimentin. J Cell Biol. 1999; 145:503–14.
44. Pekny M. Astrocytic intermediate filaments: lessons from GFAP and vimentin knock-out mice. Progressive Brain Researches. 2001; 132:23–30.
45. Faulkner JR, Herrmann JE, Woo MJ, Tansey KE, Doan NB, Sofroniew MV. Reactive astrocytes protect tissue and preserve function after spinal cord injury. Journal of Neuroscience. 2004; 24:2143–55.
46. Herrmann JE, Imura T, Song B, Qi J, Ao. Y, Nguyen TK, et al. STAT3 is a critical regulator of astrogliosis and scar formation after spinal cord injury. Journal of Neuroscience. 2008; 28:7231–43.
47. Fan H, Zhang K, Shan L, Kuang F, Chen K, Zhu K, et al. Reactive astrocytes undergo M1 microglia/macrohpages-induced necroptosis in spinal cord injury. Molecular Neurodegeneration. 2016; 11:1–16.

48. Coulson- Thomas VJ, Lauer ME, Soleman S, Zhao C, Hascall VC, Day AJ, *et al*. TSG-6 is constitutively expressed in adult CNS and associated with astrocyte-mediated glial scar formation following spinal cord injury. Journal of Biological Chemistry. 2016; 291:19939–52.
49. Milner CM, Day AJ. TSG-6: a multifunctional protein associated with inflammation. Journal of Cellular Science. 2003; 116(10):1863–73.
50. Bradbury EJ, Moon LDF, Popat RJ, King VR, Bennett GS, Patel PN, *et al*. Chondroitinase ABC promotes functional recovery after spinal cord injury. Nature. 2002; 416:636–40.
51. Massey JM, Hubscher CH, Wagoner MR, Decker JA, Amps J, Silver J, *et al*. Chondroitinase ABC digestion of the perineuronal net promotes functional collateral sprouting in the cuneate nucleus after cervical spinal cord injury. Journal of Neuroscience. 2006; 26:4406–14.
52. Carrette O, Nemade RV, Day AJ, Brickner A, Larsen WJ. TSG-6 is concentrated in the extracellular matrix of mouse cumulus oocyte complexes through hyaluronan and inter-alpha-inhibitor binding. Biological Reproduction. 2001; 65:301–8.
53. Salustri A, Yanagishita M, Hascall VC. Synthesis and accumulation of hyaluronic acid and proteoglycans in the mouse cumulus cell-oocyte complex during follicle-stimulating hormone-induced mucification. Journal of Biological Chemistry. 1989; 264:13840–7.
54. Salustri A, Yanagishita M, Underhill CB, Laurent TC, Hascall VC. Localization and synthesis of hyaluronic acid in the cumulus cells and mural granulosa cells of the preovulatory follicle. Developmental Biology. 1992; 151:541–51.
55. Camaioni A, Hascall VC, Yanagishita M, Salustri A. Effects of exogenous hyaluronic acid and serum on matrix organization and stability in the mouse cumulus cell-oocyte complex. Journal of Biol. Chemistry. 1993; 268:20473–81.
56. Fulop C. Impaired cumulus mucification and female sterility in tumor necrosis factor-induced protein-6 deficient mice. Development. 2003; 130:2253–61.
57. Stober VP, Johnson CG, Majors A, Lauer ME, Cali V, Midura RJ, *et al*. TNF stimulated gene 6 promotes formation of hyaluronan-inter-α-inhibitor heavy chain complexes necessary for ozone induced airway hyperresponsiveness. Journal of Biological Chemistry. 2017; 292:20845–58.
58. Lauer ME, Glant TT, Mikecz K, DeAngelis PL, Haller FM, Husni ME, *et al*. Irreversible heavy chain transfer to hyaluronan oligosaccharides by tumor necrosis factor-stimulated gene-6. Journal of Biological Chemistry. 2013; 288:205–14.
59. Petrey AC, De La Motte CA. Thrombin cleavage of inter-α-inhibitor heavy chain 1 regulates leukocyte binding to an inflammatory hyaluronan matrix. Journal of Biological Chemistry. 2016; 291:24324–34.
60. Hill D.R., Rho H.K., Kessler S.P., Amin R, Homer CR, McDonald C. *et al.*: Human milk hyaluronan enhances innate defense of the intestinal epithelium. Journal of Biol. Chem. 2013; 288:29090–104.
61. Baranova NS, Foulcer SJ, Briggs DC, Tilakaratna V, Enghild JJ, Milner CM. *et al.*: Inter-α-inhibitor impairs TSG-6-induced hyaluronan cross-linking. Journal of Biol. Chem. 2013; 288:29642–53.
62. Kessler S.P., Obery D.R., De La Motte C.: Hyaluronan synthase 3 null mice exhibit decreased intestinal inflammation and tissue damage in the DSS-induced colitis model. International Journal of Cell Biology. 2015.
63. Lim Y, Bendelja K, Opal S.M., Siryaporn E, Hixson D.C., Palardy J.E. Correlation between mortality and the levels of inter-alpha inhibitors in the plasma of patients with severe sepsis. Journal of Infectious Diseases. 2003; 188:919–26.
64. Schmidt E.P., Overdier K.H., Sun X., Lin L., Yang Y. *et al.*: Urinary glycosaminoglycans predict outcomes in septic shock and acute respiratory distress syndrome. American Journal of Respir. Crit Care Med. 2016; 194:439–49.
65. Coulson-Thomas VJ, Gesteira TF, Hascall V, Kao W. Umbilical cord mesenchymal stem cells suppress host rejection: the role of the glycocalyx. Journal of Biol. Chem. 2014; 289:23465–81.
66. Olté L.S., Mendichi R, Kogan G, Schiller J, Stankovská M, Arnhold J. Degradative action of reactive oxygen species on hyaluronan. 2006; Available from: https://pubs.acs.org/sharingguidelines.
67. Wight TN. Provisional matrix: a role for versican and hyaluronan [Internet]. Vols. 60–61, Matrix Biology. Elsevier B.V.; 2017 [cited 2021 Jan 15]. p. 38–56. Available from: /pmc/articles/PMC5438907/?report=abstract.

68. Cicanic M, Sykova E, Vargova L. Bral1: "Superglue" for the extracellular matrix in the brain white matter. Int. J. Biochemistry of Cell. 2012; 44:596–9.
69. Dyck SM, Karimi-Abdolrezaee S. Chondroitin sulfate proteoglycans: Key modulators in the developing and pathologic central nervous system. Exp Neurol. 2015; 269:169–87.
70. McKeon RJ, Höke A, Silver J. Injury-induced proteoglycans inhibit the potential for laminin-mediated axon growth on astrocytic scars. Exp. Neurol. 1995; 136:32–43.
71. Bradbury EJ, Carter LM. Manipulating the glial scar: chondroitinase ABC as a therapy for spinal cord injury. Brain Res Bull. 2011; 84:306–16.
72. McKeon RJ, Schreiber RC, Rudge JS, Silver J. Reduction of neurite outgrowth in a model of glial scarring following CNS injury is correlated with the expression of inhibitory molecules on reactive astrocytes. J Neuroscience. 1991; 11:3398–411.
73. Foerster AP. Spontaneous regeneration of cut axons in adult rat brain. J. Comp. Neurol. 1982; 210(4):335–56.
74. Brückner G, Bringmann A, Härtig W, Köppe G, Delpech B, Brauer K. Acute and long-lasting changes in extracellular-matrix chondroitin-sulphate proteoglycans induced by injection of chondroitinase ABC in the adult rat brain. Exp. Brain Res. 1998; 121(3):300–10.
75. Filous A.R., Miller J.H., Coulson-Thomas Y.M., Horn K.P., Alilain W.J., Silver J. Immature astrocytes promote CNS axonal regeneration when combined with chondroitinase ABC. Dev. Neurobiol. 2010; 70(12):826–41.
76. Moon LDF, Asher RA, Rhodes KE, Fawcett JW. Regeneration of CNS axons back to their target following treatment of adult rat brain with chondroitinase ABC. Nat Neurosci. 2001; 4:465–6.
77. Elkin BS, Shaik MA, Morrison B. Chondroitinase ABC reduces brain tissue swelling in vitro. J. Neurotrauma. 2011; 28(11):2277–85.
78. Busch SA, Silver J. The role of extracellular matrix in CNS regeneration. Current Opin. Neurobiol. 2007; 17:120–7.
79. Klapka N, Hermanns S, Straten G, Masanneck C, Duis S, Hamers FPT *et al.*: Suppression of fibrous scarring in spinal cord injury of rat promotes long-distance regeneration of corticospinal tract axons, rescue of primary motoneurons in somatosensory cortex and significant functional recovery. European J. of Neuroscience. 2005; 22:3047–58.
80. Milner C.M., Tongsoongnoen W, Rugg M.S, Day A.J.: The molecular basis of inter-α-inhibitor heavy chain transfer on to hyaluronan: Figure 1. Biochemistry of Soc. Trans. 2007; 35:672–6.
81. Getting S.J, Mahoney D.J, Cao T, Rugg M.S, Fries E, Milner C.M *et al.*: The link module from human TSG-6 inhibits neutrophil migration in a hyaluronan- and inter-α-inhibitor-independent manner. J. Biol. Chem. 2002; 277:51068–76.
82. Baranova N.S, Nilebäck E, Haller F.M, Briggs D.C, Svedhem S, Day A.J *et al.*: The inflammation-associated protein TSG-6 cross-links hyaluronan via hyaluronan-induced TSG-6 oligomers. J Biol Chem. 2011; 286:25675–86.
83. Higman V.A, Briggs D.C, Mahoney D.J, Blundell C.D, Sattelle B.M, Dyer D.P *et al.*: A refined model for the TSG-6 link module in complex with hyaluronan: use of defined oligosaccharides to probe structure and function. J. Biol. Chem. 2014; 289:5619–34.
84. Martin J, Midgley A, Meran S, Woods E, Bowen T, Phillips A.O *et al.*: Tumor necrosis factor-stimulated gene 6 (TSG-6)-mediated interactions with the inter-α-inhibitor heavy chain 5 facilitate tumor growth factor β1 (TGFβ1)-dependent fibroblast to myofibroblast differentiation. J. Biol. Chem. 2016; 291:13789–801
85. Franklin KBJ, Paxinos G. The mouse brain in stereotaxic coordinates (map). Boston: Academic Press; 2007